NACA

RESEARCH MEMORANDUM

EXPERIMENTAL INVESTIGATION OF THRUST AUGMENTATION OF

4000-POUND-THRUST CENTRIFUGAL-FLOW-TYPE

TURBOJET ENGINE BY BLEEDOFF

By William L. Jones and Louis J. Bogdan

Lewis Flight Propulsion Laboratory
Cleveland, Ohio

NATIONAL ADVISORY COMMITTEE
FOR AERONAUTICS
WASHINGTON
July 3, 1950

NATIONAL ADVISORY COMMITTEE FOR AERONAUTICS

RESEARCH MEMORANDUM

EXPERIMENTAL INVESTIGATION OF THRUST AUGMENTATION OF

4000-POUND-THRUST CENTRIFUGAL-FLOW-TYPE

TURBOJET ENGINE BY BLEEDOFF

By William L. Jones and Louis J. Bogdan

SUMMARY

An experimental investigation of thrust augmentation by bleedoff was conducted on a 4000-pound-thrust turbojet engine at zero flight-speed, sea-level conditions. In the bleedoff cycle, secondary combustion air was bled off from the combustion chambers, heated in an auxiliary combustion-chamber, and discharged through an exhaust nozzle. Water was injected into the combustion chambers to replace the bleed-off air; water and alcohol were injected at the compressor inlets.

This method of thrust augmentation provided very high thrust increases at the expense of high liquid consumption. An augmented thrust of nearly 1.8 times the normal thrust was obtained with a total liquid flow about 13 times the unaugmented engine fuel flow. For successful bleedoff-cycle operation, it was necessary that a proper balance or equilibrium of the several engine operating variables be maintained within very narrow limits.

INTRODUCTION

As a part of a general research program to investigate various methods of thrust augmentation of turbojet engines, an investigation of the performance of the bleedoff cycle on a 4000-pound-thrust centrifugal-flow-type turbojet engine has been conducted at the NACA Lewis laboratory and the results are presented herein.

In the air bleedoff cycle, the secondary-combustion or excess air, which is normally required to prevent the turbine-inlet temperature from exceeding permissible values, is bled off from the combustion chambers and ducted to a bleedoff combustor where it is heated to a high temperature and discharged through an exhaust nozzle. The air that is bled off is replaced by water that is

injected into and vaporized in the combustion chambers and passes
through the turbine as steam. Thus, in essence, the excess air is
replaced by steam and at the same time a high-pressure air supply
for an auxiliary jet is made available. Water and alcohol are
injected at the compressor inlets; this injection is considered a
part of the bleedoff cycle and is incorporated to provide an increase
in compressor-outlet pressure and mass flow.

For convenience of terminology, the bleedoff engine is consid-
ered to consist of two main components, the standard turbojet engine
and a bleedoff combustor, which are hereinafter referred to as "the
primary and secondary engines," respectively.

An investigation of the performance of the bleedoff cycle con-
ducted on a 1600-pound-thrust centrifugal-flow-type turbojet engine
over a limited range of test conditions is reported in reference 1.
The results of this investigation indicate that thrust augmentation
as high as predicted by theoretical analysis could be realized.

The investigation on a 4000-pound-thrust centrifugal-flow-type
turbojet engine was conducted to extend the range of conditions
investigated in reference 1. This investigation was made at zero
flight-speed, sea-level conditions and at approximately rated engine
speed and tail-pipe temperature. The bleedoff weight flows ranged
up to 31 percent of normal compressor air flow (without inlet injec-
tion or bleedoff). Various size exhaust nozzles were used on the
secondary engine and a fixed-area exhaust nozzle was used on the
primary engine.

Performance curves and data analysis are presented that provide
an insight into the operating characteristics of the bleedoff cycle
and illustrate the thrust augmentation obtainable at various oper-
ating conditions.

APPARATUS

General Setup

The general arrangement of the bleedoff engine installation is
shown in figure 1. The primary engine used was a double-entry
centrifugal-flow-type turbojet engine (J33) having 14 can-type com-
bustion chambers and a nominal thrust rating of 4000 pounds at rated
engine speed of 11,500 rpm. The engine was rigidly mounted on a
frame that was suspended from the ceiling of the test cell by four
rods swinging on ball-bearing pivots. Lateral restraint was provided

by guide rollers; longitudinal restraint was provided by the thrust-measuring device. All instrumentation and control lines were flexible and a special seal (detail A in fig. 1) was installed where the primary engine tail pipe and the bleedoff ducting passed through the wall of the cell in order to reduce air leakage into the nearly airtight test cell. The fuel used, AN-F-32, was measured with calibrated rotameters. The engine combustion-air flow entered the test cell through two air-metering nozzles designed according to A.S.M.E. specifications having a 53-inch-diameter approach section and an 18-inch-diameter throat. The total thrust, produced by both the primary and secondary engines, was measured by a calibrated air balancing thrust cell and the thrust of the primary engine alone was measured by means of a tail rake installed at the primary engine exhaust-nozzle exit. A 19.5-inch-diameter fixed-area conical exhaust-nozzle was used on the primary engine.

Injection and Bleedoff Equipment

The injection of water and alcohol into the compressor inlets was accomplished by means of 84 flat-spray-type nozzles equally spaced circumferentially around the inlets; 14 nozzles were used for alcohol and 28 nozzles for water at each of the compressor inlets. The injection of water into the primary-engine combustion chambers was effected by means of 56 injection nozzles; four nozzles were placed circumferentially around each combustion chamber, one nozzle on the inner periphery of the combustion-chamber assembly and the other three on the outside, as shown in figure 2. The nozzles were located in a single plane midway axially along the combustion chamber.

Water and alcohol flows were measured by means of calibrated orifices. The alcohol used was a mixture of 50-percent methyl and 50-percent ethyl alcohol by weight.

The bleedoff equipment (the secondary engine), shown in figures 2 to 4, consisted of (a) a bleedoff manifold, (b) ducting, and (c) a bleedoff combustor and exhaust nozzle. The bleedoff manifold had a rectangular cross section and was wrapped around the primary-engine combustion chambers. Slots were provided in each combustion chamber through which secondary-combustion air was bled off. The cross-sectional area of the manifold progressively increased as it passed successive combustion chambers, which tended to equalize the amount of air bled off from each combustion chamber.

The bleedoff ducting contained: (a) a butterfly valve to control the bleedoff air flow, (b) a honeycomb to straighten out the flow, (c) an air-measuring nozzle designed according to A.S.M.E. specifications using an 8-inch-diameter approach section and a $5\frac{1}{2}$-inch-diameter throat, and (d) a diffuser.

The bleedoff combustor, shown in figure 4, was intended primarily as a research instrument, thus no effort was made to minimize either its size or weight. This combustor consisted essentially of a pilot-burner section and a main combustion section. The pilot-burner section contained a single cone-spray-type fuel nozzle, a spark plug, a standard inner liner and combustion dome of a 1600-pound-thrust turbojet engine (J31), and a star-shaped baffle to create turbulence for better mixing. Immediately downstream of the baffle at the entrance to the combustion section were located two main fuel manifolds. The forward manifold contained twelve flat-spray-type nozzles and the aft manifold contained six cone-spray-type nozzles. A V-gutter-type flame-holder with a gutter width of 1.5 inches and a mean diameter of 9 inches was located downstream of the fuel-injection manifolds. The combustion section was 14 inches in diameter and 30 inches long and was cooled by a water jacket. Water to this jacket was admitted at the upstream end of the combustion section and discharged into the exhaust gas of the bleedoff combustor through a series of holes at the entrance to the exhaust nozzle. A series of conical exhaust nozzles varying from 4.5 to 7.0 inches in diameter were used during the investigation.

PRESSURE AND TEMPERATURE INSTRUMENTATION

Primary Engine

The stations at which the primary engine was instrumented for pressure and temperature measurements are shown in figure 3. The variables measured and the number, type, and location of the instruments are:

(1) Cowling-inlet total temperature, T_0, average of five groups of four thermocouples in parallel in cowling inlet

(2) Inlet-air total pressure, P_0, one open-end tube in quiescent zone of test cell

(3) Compressor-outlet total temperature, T_2, average of three separately read unshielded thermocouples each located in a different diffuser elbow

(4) Compressor-outlet total pressure, P_2, average of two separately read total head tubes each in a different diffuser elbow

(5) Turbine-outlet gas total temperature, T_5, six thermocouple rakes, of six thermocouples each, spaced in groups of two (one rake between two combustion chambers and the other rake on the center line of adjacent combustion chamber) about 120° apart and each thermocouple individually recorded on a flight recorder

(6) Tail-pipe gas total temperature, T_7, four strut-type thermocouples located slightly upstream of the exhaust nozzle and read both individually and in parallel

(7) Exhaust-nozzle static and total pressure, p_8 and P_8, measured by a jet rake containing four static tubes and ten total head tubes.

Bleedoff System

The stations at which the bleedoff system was instrumented for pressure and temperature measurements are also shown in figure 3. The variables measured and the number, type, and location of instruments are:

(1) Bleedoff-air static pressure, p_9, four wall statics connected in parallel and located at the air measuring-nozzle

(2) Bleedoff-air total pressure, P_9, one total head tube located in the center of the air stream at the air-measuring-nozzle throat

(3) Bleedoff-air total temperature, T_9, one open-type thermocouple located at the air-measuring-nozzle throat.

PROCEDURE

Operating Conditions

For all bleedoff runs, an attempt was made to operate the primary engine at rated speed (11,500 rpm) and tail-pipe gas temperature (1680° R). Difficulty was experienced, however, in obtaining precisely

controlled test conditions because of the necessity of close coordi-
nation of control and equilibrium between the many variables for
satisfactory operation. Accordingly, the operating conditions for
which data were obtained were somewhat different for various runs.
The range of corrected conditions (discussed later) at which data
were obtained is shown in the following table:

Bleedoff-nozzle diameter (in.)	Engine speed (rpm)	Combustion-chamber, water injection (lb/sec)	Bleedoff weight flow (lb/sec)	Secondary-engine fuel flow (lb/sec)	Primary engine tail-pipe temperature ($^{\circ}$R)
4.5	11,603-11,658	3.78-4.10	12.3-12.8	0.125-.185	1675-1681
5.0	11,655	4.73-5.14	12.6-12.9	.300-.366	1693
5.5	11,614	6.24	14.2	.415	1660
6.0	11,270	9.12	16.0	.589	1604
7.0	11,160-11,496	2.83-8.07	10.5-21.4	.565-1.220	1659-1693

All data were obtained with the butterfly valve in a wide-open
position. For a given primary-engine operating speed and tail-pipe
temperature, the bleedoff weight flow was therefore, dependent only
on the bleedoff-nozzle size and secondary engine fuel flow. The
primary-engine combustion-chamber water-injection flow is not an
independent variable but is the amount required to maintain rated
engine conditions at the given bleedoff weight flow. Inasmuch as
the purpose of this investigation was to obtain the maximum thrust
in the secondary engine, that could be obtained at stoichiometric
fuel-air ratio with the largest nozzle size (and bleedoff flow),
the scope of effort on the smaller nozzle sizes was limited. The
injection of water and alcohol at the compressor inlets was held
approximately constant at 2.0 and 2.2 pounds per second, respec-
tively, for all bleedoff runs. These values for the water and
alcohol flows were chosen as they produced high thrust augmentation
due to inlet injection without excessive total specific liquid
consumption (reference 2).

Operating Procedure

For successful bleedoff cycle operation, it was necessary that
a proper balance or equilibrium among the various operating variables

be maintained within very narrow limits if the engine were to operate satisfactorily at any condition. For example, at a given engine speed and bleedoff flow, an oversupply of water would either cause combustion to cease or reduce the turbine-inlet temperature so that the turbine could not maintain speed (resulting in primary engine deceleration to the point of combustion failure) or cause compressor surge. On the other hand, an undersupply of water would result in excessive tail-pipe temperatures. Therefore, as the bleedoff butterfly valve was opened, it was necessary to increase both the primary and secondary fuel flow and the water injection simultaneously and in proper balance with the increasing bleedoff flow.

In general, bleedoff operation was started at an engine speed of about 11,000 rpm and as the butterfly valve was gradually opened the water and fuel flows were gradually increased using engine speed and temperature as an operating guide. Then, after the valve was fully opened, the engine speed was gradually increased, simultaneously with further increases in water and fuel flows, until what was considered a satisfactory operating point was reached.

SYMBOLS

The following symbols are used in the equations in this report:

A   area, (sq in.)

$C_1, \ldots C_5$ constants

F   thrust, (lb)

F_a total augmented thrust $(F_e + F_b)$, (lb)

f/a   fuel-air ratio

g   acceleration due to gravity, (ft/sec^2)

N   engine speed, (rpm)

P   total pressure, (lb/sq in.)

p   static pressure, (lb/sq in.)

R   gas constant, (ft-lb/lb °R)

T	total temperature, (°R)
V	jet velocity, (ft/sec)
W	weight flow, no fuel, (air, water, and alcohol), (lb/sec)
W_a	air flow, (lb/sec)
W_{al}	alcohol flow, (lb/sec)
$\dot{W}_f$	fuel flow, (lb/sec)
W_l	total liquid flow, (fuel, water, and alcohol), (lb/sec)
W_{tot}	total weight flow, (fuel, air, water, and alcohol), (lb/sec)
W_w	water flow, (lb/sec)
γ	ratio of specific heats
η	combustion efficiency

Subscripts:

0	cowling inlet or ambient
2	compressor outlet
5	turbine outlet
7	tail pipe
8	primary-engine exhaust-nozzle outlet
9	bleedoff air-metering nozzle
11	bleedoff exhaust-nozzle inlet
12	bleedoff exhaust-nozzle outlet
b	bleedoff
c	primary-engine combustion chambers

i   compressor inlets

n   normal

p   primary engine

s   secondary engine

ANALYSIS OF DATA

The performance data were corrected to NACA standard inlet-air pressure and temperature conditions of 14.7 pounds per square inch absolute and 519° R, respectively, by means of the following factors:

$\dfrac{F_p}{\delta}, \dfrac{F_s}{\delta}$ corrected thrust

$\dfrac{N}{\sqrt{\theta}}$ corrected speed

$\dfrac{P}{\delta}$ corrected pressure

$\dfrac{T}{\theta}$ corrected temperature

$\dfrac{W_{a,b}\sqrt{\theta}}{\delta}, \dfrac{W_{a,p}\sqrt{\theta}}{\delta}$ corrected air flow

$\dfrac{W_{al}\sqrt{\theta}}{\delta}$ corrected alcohol flow

$\dfrac{W_{f,s}K_b}{\delta\sqrt{\theta}}$ corrected secondary-engine fuel flow

$\dfrac{W_{f,p}}{\delta\sqrt{\theta}}$ corrected primary-engine fuel flow

$\dfrac{W_w\sqrt{\theta}}{\delta}$ corrected water flow

where

$$\delta = \frac{\text{cowling-inlet total pressure, } P_0, \text{ (lb/sq in. abs.)}}{\text{NACA standard sea-level pressure, 14.7 (lb/sq in. abs.)}}$$

$$\theta = \frac{\text{cowling-inlet total temperature, } T_0, \text{ }^\circ R}{\text{NACA standard sea-level temperature, 519}^\circ \text{ R}}$$

$$K_s = 1 + \frac{0.553 \text{ } W_{al,b}}{W_{fs}}, \text{ correction factor for secondary-engine}$$
fuel flow

Except for the factors for corrected water, alcohol, and secondary-engine fuel flow, the method of correction shown here is the same as discussed in references 3 and 4. The injected water and alcohol flows are corrected in the same manner as the air flow so that the water-air and alcohol-air ratios are the same before and after correction. The alcohol flow to the secondary engine $W_{al,b}$ was taken equal to the alcohol injected at the compressor inlets $W_{al,i}$ times the ratio of the bleedoff weight flow to the compressor weight flow W_b/W_p. For convenience of application, the effect of alcohol as fuel is considered as a correction factor K_s on the secondary-engine fuel flow. The constant 0.553 appearing in the correction factor K_s represents the ratio of the effective heating value of the alcohol to the effective heating value of the fuel (kerosene). This factor K_s is used for the computation of the fuel-air ratios of the secondary engine. A similar correction factor for the primary-engine fuel flow is not required because the fuel-air ratios of the primary engine are not presented herein.

A theoretical analysis of the wet-compression process (reference 5) indicated that over a limited range of inlet conditions for a given compressor Mach number and water-air or alcohol-air ratio, the compressor-outlet pressure and temperature are nearly proportional to inlet pressure and temperature. Although the correction factors P/δ and T/θ are therefore satisfied for the small range of inlet conditions encountered in the present investigation, they should not be used to extrapolate the present data to altitude conditions without further experimental verification. The primary-engine fuel flow was corrected only by the conventional correction factors for changes in inlet conditions. Because the flow of alcohol

(which acts as fuel in the primary-engine combustion chambers) was corrected differently than the kerosene flow, an additional correction to the kerosene flow, such as used in reference 1, is required to maintain a heat balance before and after correction. This correction is omitted herein because the range of inlet conditions was small and the correction was negligible.

All experimental augmentation results were based on normal performance runs determined immediately before each augmentation run. Because the data were obtained at slightly different corrected engine speeds adjustment was made to reduce the results to a constant engine speed of 11,600 rpm by use of empirical relations derived from data analysis as most of the data were obtained at that speed.

RESULTS AND DISCUSSION

The primary-engine tail-pipe gas temperature and exhaust-nozzle area were maintained constant; therefore, a fixed relation existed between the water injection rate to the primary-engine combustion chambers and the bleedoff weight flow. Figure 5 shows that this relation is linear and about 0.37 pound of water is required to replace each pound of bleedoff weight flow. Thus, with a bleedoff weight flow of 24 pounds per second, (about 31 percent of normal compressor air flow) about 9 pounds of water per second must be injected into the primary-engine combustion chambers.

In order to vaporize and to superheat the injected water, additional fuel must be burned in the primary-engine combustion chambers. Although a part of this fuel is supplied by the alcohol injected at the compressor inlets, additional kerosene was required for the higher bleedoff rates. The relation of fuel flow (kerosene) to the primary-engine combustion chambers to the bleedoff weight flow is shown in figure 6. The fuel flow increases from about 1.0 pound per second at no bleedoff flow to 2.0 pounds per second at a bleedoff flow of 24 pounds per second.

Also shown in figure 6 is the normal fuel flow (1.25 lb/sec), which is somewhat higher than the fuel flow with no bleedoff. Reduction in fuel flow at the condition of no bleedoff is caused by combustion of the alcohol that was injected with water at the compressor inlet for the bleedoff runs.

Further increases in the bleedoff weight flow above the maximum
of about 24 pounds per second shown in figures 5 and 6 resulted in
combustion failure in the primary engine. At this bleedoff flow,
the over-all fuel-air ratio including alcohol in the primary-engine
combustion chambers was about 0.032. Although this over-all fuel-
air ratio is considerably below over-all stoichiometric fuel-air
ratio, the fuel-air ratio in the primary combustion zone was, of
course, much richer and the combustion failure was possibly the
result of rich blow-out. Satisfactory operation at higher bleedoff
flows will therefore require design changes in the primary-engine
combustion chambers.

The individual liquid flows to the primary engine are shown in
figure 7 as a function of bleedoff weight flow. As previously
illustrated, when the bleedoff weight flow increased, the fuel flow
and water flow to the primary-engine combustion chambers increased.
The water and alcohol injection to the compressor inlets was held
constant and is shown as a horizontal straight line; this line rep-
resents an average of the actual data points, which have been omitted
for clarity in the figure. The net result of these three flows is an
increase in the total liquid flow into the primary engine with
increased bleedoff weight flow, as shown by the upper fuel-flow curve.
The total liquid flow to the primary engine increases from about
5 pounds per second at no bleedoff to about 15 pounds per second at
a bleedoff weight flow of 24 pounds per second. The increase in
total liquid flow to the primary engine is less than the increase
in bleedoff weight flow; therefore, the net result is a decrease in
total flow through the turbine and primary-engine exhaust jet. This
effect more than offsets any favorable effects of the change in
thermodynamic properties of the working fluid and consequently, there
is a small reduction in the augmented primary-engine thrust, as shown
by the curve at the top of figure 7. The ratio of augmented primary-
engine thrust to normal engine thrust thus decreased from about 1.26
at no bleedoff (but with inlet injection) to about 1.15 at a bleedoff
weight flow of 24 pounds per second.

The change in air flow through the compressor with bleedoff
flow was very small. For example, at 11,600 rpm the compressor air
flow increased from about 83.5 pounds per second at no bleedoff to
about 84.5 pounds per second at a bleedoff weight flow of 24 pounds
per second.

The performance of the secondary engine is analyzed in two
parts, the total weight flow and the thrust. In order to provide
an insight into the effects of the operating variables on these

performance variables, the total weight flow and thrust have been plotted in the form of parameters, which are derived in the appendix from fundamental flow equations.

It is shown in the appendix that the total weight-flow parameter $W_{tot,b}/P_9A_{12}$ (from equation (3) in the appendix) is a function of fuel-air ratio and combustion efficiency. This parameter is plotted against the fuel-air ratio of the secondary engine in figure 8. The total weight-flow parameter decreases rapidly as the fuel-air ratio increases from 0.025 to 0.050 and then becomes nearly constant with a further increase in fuel-air ratio. The dashed line in the figure is the calculated ideal curve assuming a combustion efficiency of 100 percent, a nozzle flow coefficient of 1.0, and zero pressure drop in the secondary engine combustor. As previously discussed, cooling water was injected into the secondary engine at the exhaust-nozzle inlet. This cooling-water flow was very small in comparison to the bleedoff flow, however, and its effect on secondary-engine thrust was neglected in the calculations. A greater total-weight-flow parameter was experimentally obtained for a given fuel-air ratio than the theoretical curve predicts because of higher total weight flows associated with lower combustion temperatures due to combustion inefficiency. As can be seen in figure 8, the data correlate satisfactorily and thus the bleedoff total weight flow can be determined from this correlation curve for any bleedoff pressure, exhaust-nozzle area, and secondary-engine fuel-air ratio.

Values of the thrust parameter $F_s/P_9A_{12} + p_0/P_9$ (from equation (10) in the appendix) calculated from the experimental data are plotted against secondary-engine nozzle area in figure 9. The value of the thrust parameter is 1.18 (as compared to a theoretical value of 1.25) for secondary-engine nozzle sizes varying from 4.5 to 7.0 inches in diameter (corresponding to areas from about 16 to 39 sq in.). With the constant value of this parameter, the thrust of the secondary engine may be calculated for any value of the inlet pressure, ambient pressure, and nozzle area.

Plots of secondary-engine thrust, primary-engine thrust, and total augmented thrust to normal thrust ratios against bleedoff weight flow are presented in figure 10. The dashed lines in the lower portion of the figure are the ratio of secondary-engine thrust to normal-engine thrust calculated from the correlation curves shown in figures 8 and 9, and for values of p_0/P_9 representative of test conditions, and for secondary-engine fuel-air ratios of 0.03, 0.05, and 0.08. Although the data were not obtained at three different

constant fuel-air ratios, the range covered was such that the data may be grouped into three approximately constant values of 0.03, 0.05, and 0.08 and are so coded in the figure. The analysis has therefore permitted intelligent separation of the data showing the effect of fuel-air ratio, which otherwise would have been obscured by the scatter of data. An increase in fuel-air ratio is seen to increase thrust. The greatest increase in thrust occurs with an increase of the secondary-engine fuel-air ratio from 0.03 to 0.05, with a smaller thrust increase as the fuel-air ratio increases from 0.05 to 0.08.

Also plotted in figure 10 is the ratio of primary-engine thrust to normal-engine thrust previously presented in figure 7. The ratio of total augmented thrust (sum of primary- and secondary-engine thrust) to normal thrust, hereinafter referred to as "the augmented thrust ratio," is plotted against bleedoff weight flow in the top portion of figure 10.

Although the primary-engine thrust decreased with increasing bleedoff flow, the predominate contribution of the secondary engine results in an increase of augmented thrust ratio with both increasing bleedoff flow and secondary fuel-air ratio. The augmented thrust ratio increases linearly with bleedoff flow and reaches a value of approximately 1.8 at a bleedoff flow of 24 pounds per second and a secondary-engine fuel-air ratio of 0.08.

The augmented thrust ratio is replotted in figure 11 as a function of augmented liquid ratio (ratio of total liquid flows to primary and secondary engines to normal-engine fuel flow). The experimental points shown are coded for the appropriate ranges of secondary-engine fuel-air ratios, as in figure 10. The solid lines in figure 11 were obtained by cross-plotting the thrust curves of figure 10 with curves of total liquid flow (not shown) based on the primary-engine total liquid flow presented in figure 7, and the computed secondary-engine fuel flows for fuel-air ratios of 0.03, 0.05, and 0.08. The dashed curve was obtained in a similar manner from figures 8 and 9 for 100-percent combustion efficiency and stoichiometric mixture in the secondary engine. The experimental results agree within 5 percent with the values calculated from the correlation curves. The augmented-thrust ratio is shown to increase linearly with the augmented liquid flow ratio. For a given thrust ratio, the augmented liquid flow ratio decreases considerably as the secondary-engine fuel-air ratio increases from 0.03 to 0.05. A further increase in fuel-air ratio from 0.05 to 0.08 results in a slight increase in augmented liquid flow ratio. In addition to reducing the augmented liquid flow ratio, operation at a high

secondary-engine fuel-air ratio also results in a lower bleedoff weight flow, which is desirable from the standpoint of combustion in the primary engine. The maximum augmented thrust ratio experimentally obtained was about 1.8 at a liquid flow ratio of about 13.0, or a total liquid flow of about 17 pounds per second, as compared to a total augmented thrust ratio obtainable with an ideal secondary engine of about 2.0.

SUMMARY OF RESULTS

The following results were obtained from a thrust-augmentation investigation on a 4000-pound-thrust centrifugal-flow-type turbojet engine by air bleedoff at zero flight-speed, sea-level conditions:

1. The maximum ratio of augmented thrust to normal-engine thrust experimentally obtained was about 1.8 at a bleedoff flow of 24 pounds per second and a total liquid flow of 17 pounds per second.

2. The maximum bleedoff flow was limited by primary-engine combustion failure, which occurred at a bleedoff flow of about 24 pounds per second or 31 percent of the normal compressor air flow.

3. For each pound of air bled off, it was necessary to inject 0.37 pound of water into the primary-engine combustion chambers to maintain normal engine speed (11,500 rpm) and tail-pipe temperature (1680° R).

4. For successful bleedoff-cycle operation, it was necessary that a proper balance or equilibrium of the several engine operating variables be maintained within very narrow limits.

Lewis Flight Propulsion Laboratory,
    National Advisory Committee for Aeronautics,
        Cleveland, Ohio.

APPENDIX - METHOD OF DATA CORRELATION

In order to provide a better understanding of the effects of the operating variables on the performance of the secondary engine, the weight flow and thrust are expressed in the form of parameters derived from fundamental flow equations. For a convergent nozzle operating at greater than critical pressure ratio,

$$W_{tot,b} = C_1 \frac{P_{12}A_{12}}{\sqrt{T_{12}}} \tag{1}$$

Because the pressure drop through the bleedoff combustor is small, the assumption is made that

$$\frac{P_9}{P_{12}} = C_2 \tag{1a}$$

Substituting equation (1a) in equation (1) and dividing through by P_9A_{12} yields,

$$\frac{W_{tot,b}}{P_9A_{12}} = \frac{C_3}{\sqrt{T_{12}}} \tag{2}$$

For a constant inlet temperature, T_9, $\sqrt{T_{12}}$ may be replaced by a function of the fuel-air ratio and combustion efficiency. Hence,

$$\frac{W_{tot,b}}{P_9A_{12}} = C_3, \left\{ f\left[(f/a)_b, \eta_B\right] \right\} \tag{3}$$

The thrust of a convergent nozzle operating at the supercritical pressure ratio may be expressed as

$$F_s = W_{tot,b} V_{12} + (P_{12} - P_0) A_{12} \tag{4}$$

Dividing through by $P_{12}A_{12}$ and rearranging yields

$$\frac{F_s}{P_{12}A_{12}} + \frac{P_0}{P_{12}} = \frac{W_{tot,b} V_{12}}{P_{12}A_{12}} + 1 \tag{5}$$

For a convergent nozzle operating with inlet pressures equal to or greater than the critical pressure, the nozzle-outlet total pressure is equal to a constant times the outlet static pressure. Therefore,

$$C_4 p_{12} = P_{12} \tag{6}$$

By substituting P_{12} from equation (1a) in equation (6)

$$p_{12} = \frac{P_9}{C_5} \tag{6a}$$

By replacing p_{12} with P_9/C_5 in equation (5)

$$\frac{F_s}{P_9 A_{12}} + \frac{p_0}{P_9} = \frac{W_{tot,b}\, V_{12}}{P_9 A_{12}} + \frac{1}{C_5} \tag{7}$$

Also, because the nozzle-outlet velocity is equal to sonic velocity,

$$V_{12} = \sqrt{\frac{2\gamma}{\gamma + 1}\, gRT_{12}} \tag{8}$$

Substitution of equations (2) and (8) into equation (7) gives

$$\frac{F_s}{P_9 A_{12}} + \frac{p_0}{P_9} = \frac{C_3}{\sqrt{T_{12}}} \sqrt{\frac{2\gamma}{\gamma + 1}\, gRT_{12}} + \frac{1}{C_5} \tag{9}$$

consequently, neglecting changes in γ and R

$$\frac{F_s}{P_9 A_{12}} + \frac{p_0}{P_9} = \text{constant} \tag{10}$$

REFERENCES

1. Hall, Eldon W.: Thrust-Augmentation Tests of Type I-16 Jet-Propulsion Engine by Bleedoff and Water and Alcohol Injection. NACA MR E5H24, 1945.

2. Jones, William L., and Engelman, Helmuth W.: Experimental Investigation of Thrust Augmentation of 4000-Pound-Thrust Centrifugal-Flow-Type Turbojet Engine by Injection of Water and Alcohol at Compressor Inlets. NACA RM E7J19, 1948.

3. Warner, D. F. and Auyer, E. L.: Contemporary Jet-Propulsion Gas Turbines for Aircraft. Mech. Eng., vol. 67, no. 11, Nov. 1945, pp. 707-714.

4. Sanders, Newell D.: Performance Parameters for Jet-Propuslion Engines. NACA TN 1106, 1946.

5. Trout, Arthur M.: Theoretical Turbojet Thrust Augmentation by Evaporation of Water During Compression as Determined by Use of a Mollier Diagram. NACA TN 2104, 1950.
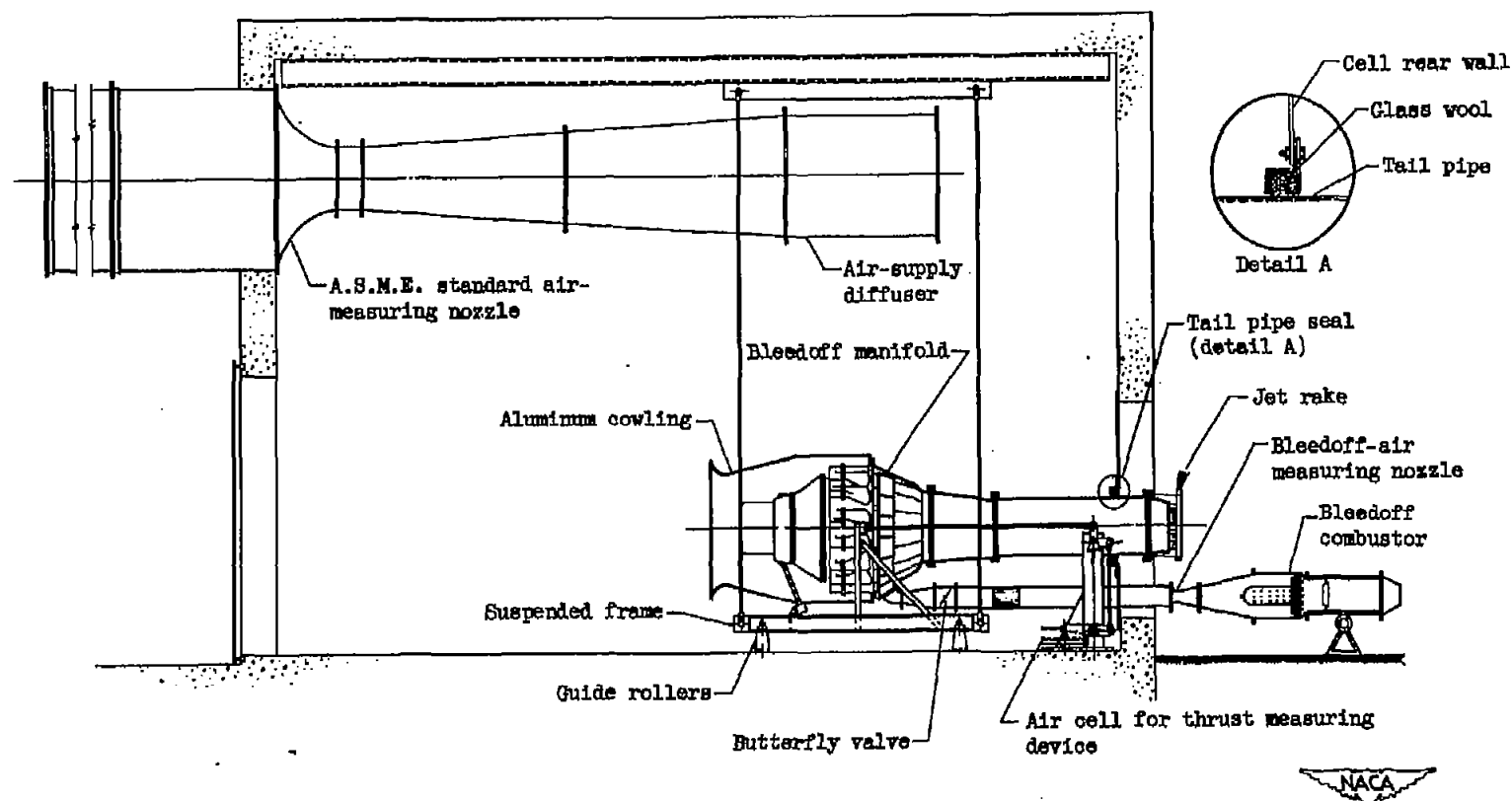
Figure 1. - Diagram of setup for investigation of turbojet engine performance with bleedoff.
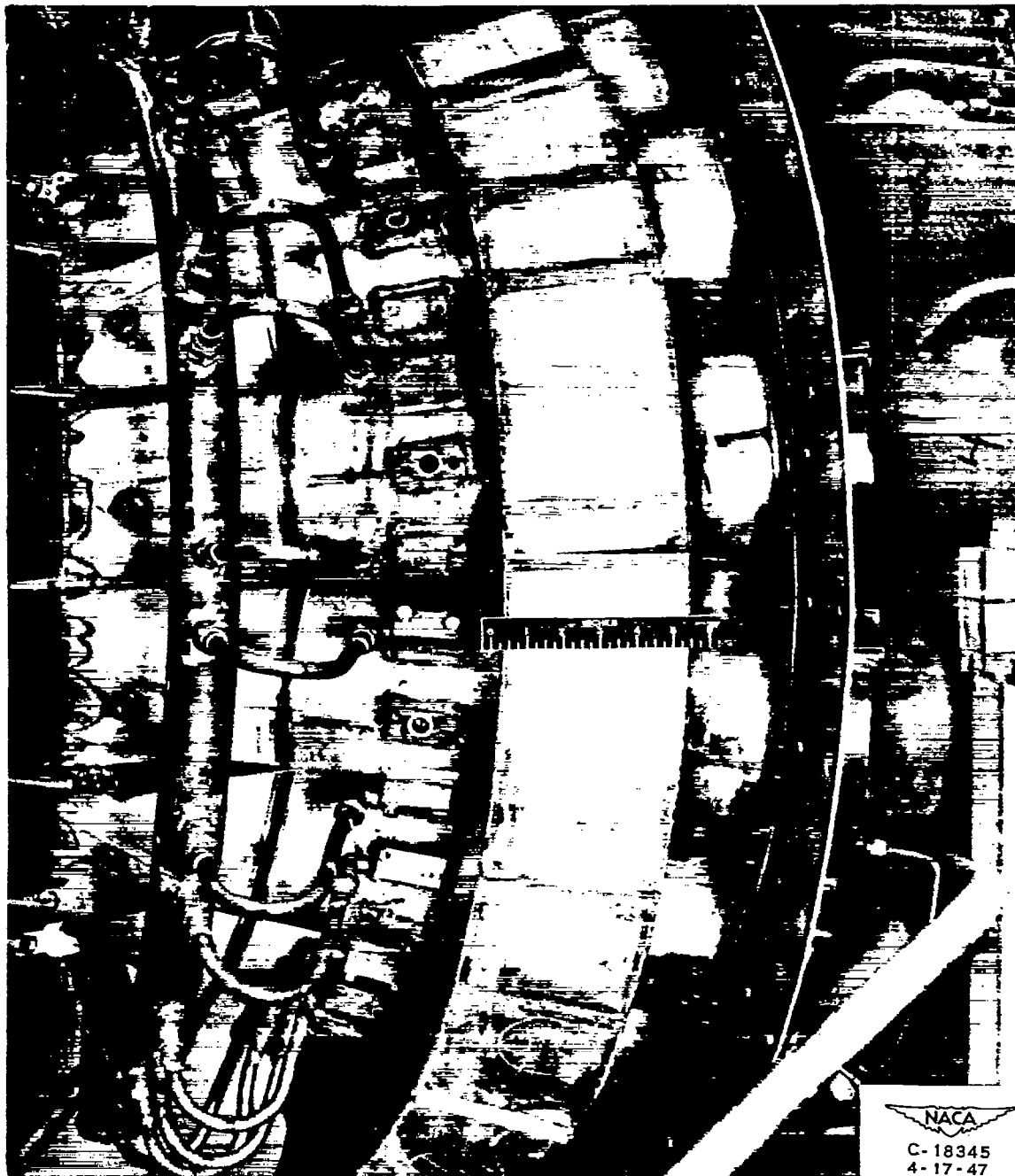
Figure 2. - Combustor section of primary engine showing bleedoff manifold and combustion-
chamber injection equipment.
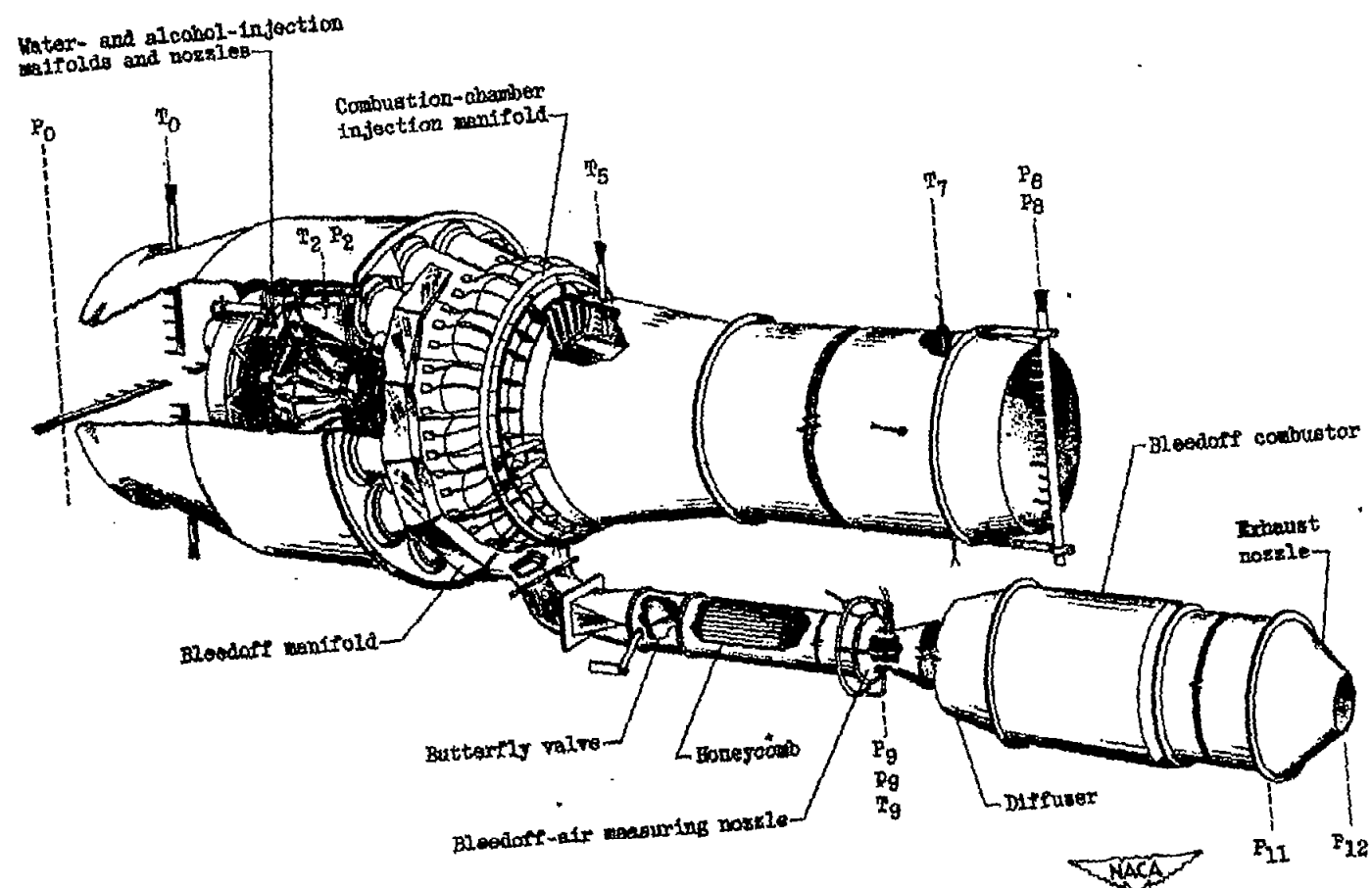
Figure 3. - Instrumentation, injection, and bleedoff equipment for investigation of engine performance with bleedoff on turbojet engine.
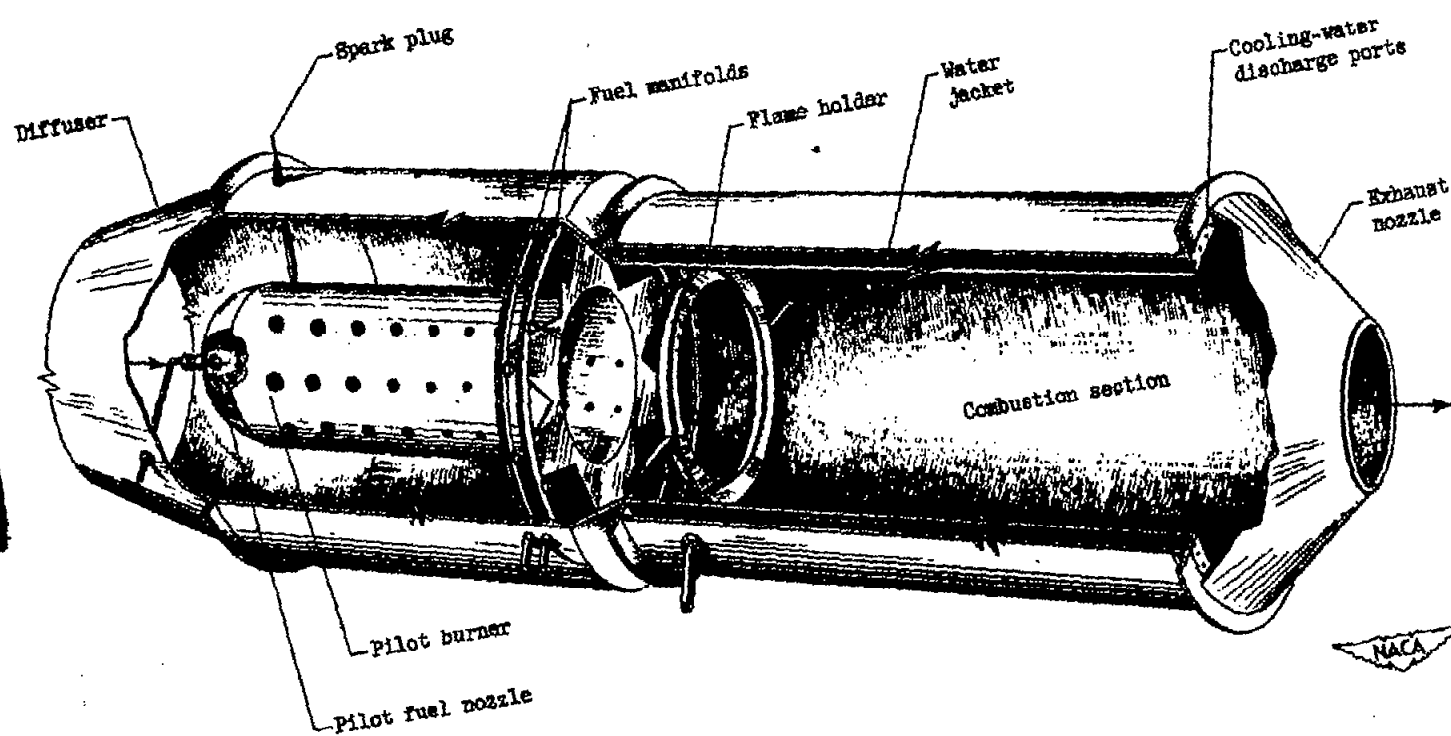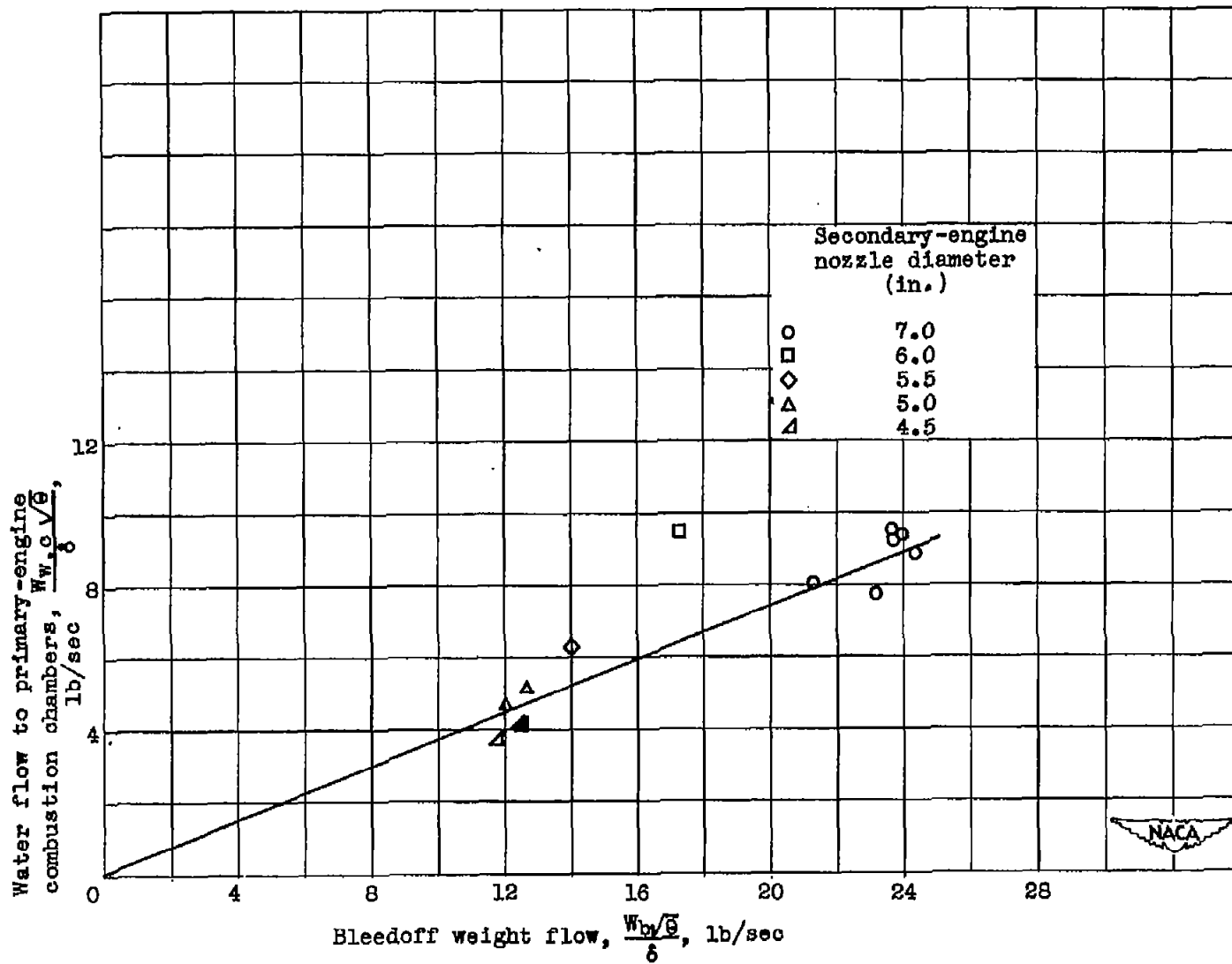
Figure 4. - Schematic sketch of bleedoff combustor.

Spark plug

Diffuser

Fuel manifolds

Flame holder

Water jacket

Cooling-water discharge ports

Exhaust nozzle

Combustion section

Pilot burner

Pilot fuel nozzle

NACA

NACA RM E50D17

Figure 5. - Variation of water flow to primary-engine combustion chambers with bleedoff weight flow.
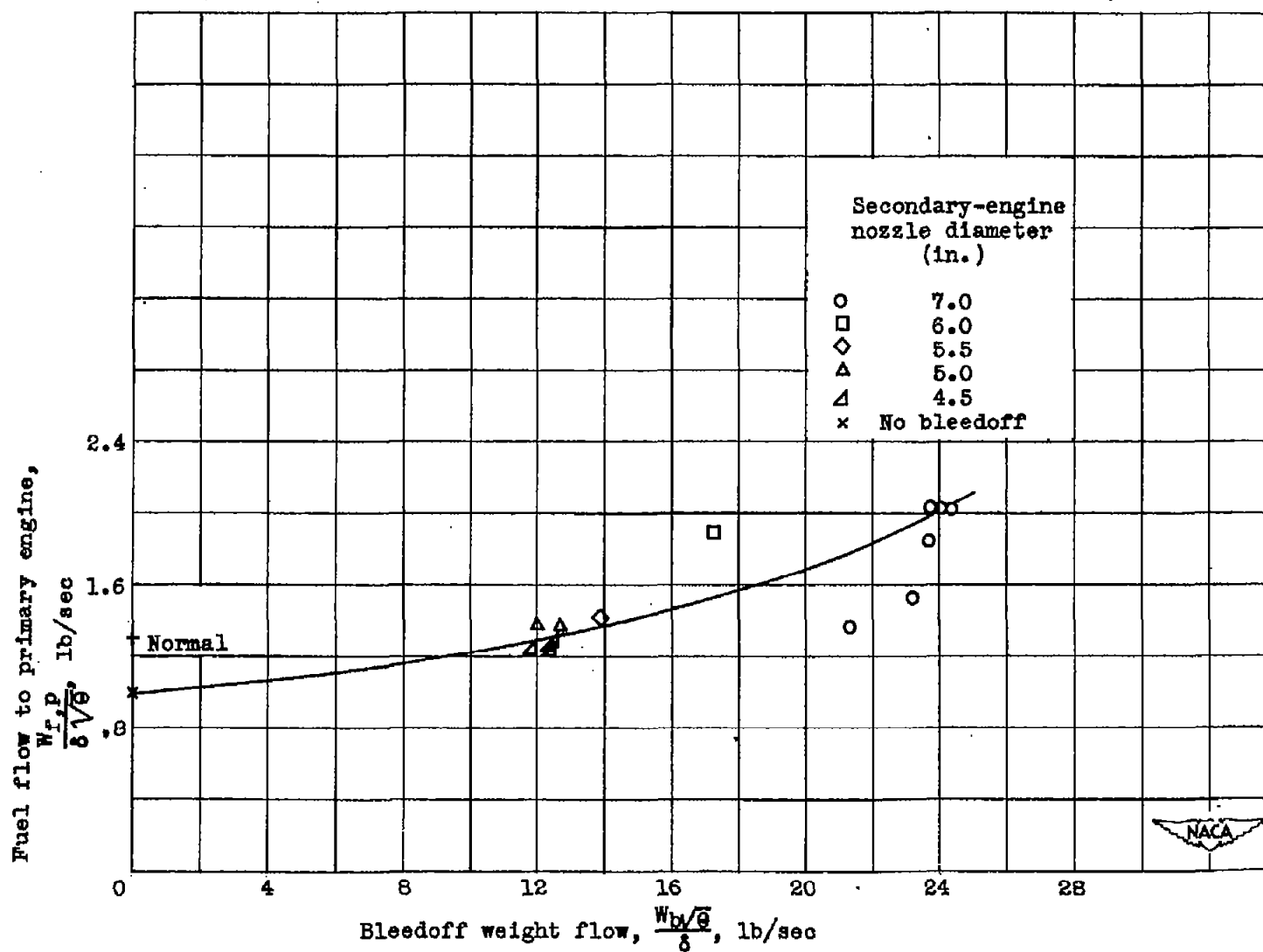
Figure 6. - Variation of fuel flow to primary engine with bleedoff weight flow.
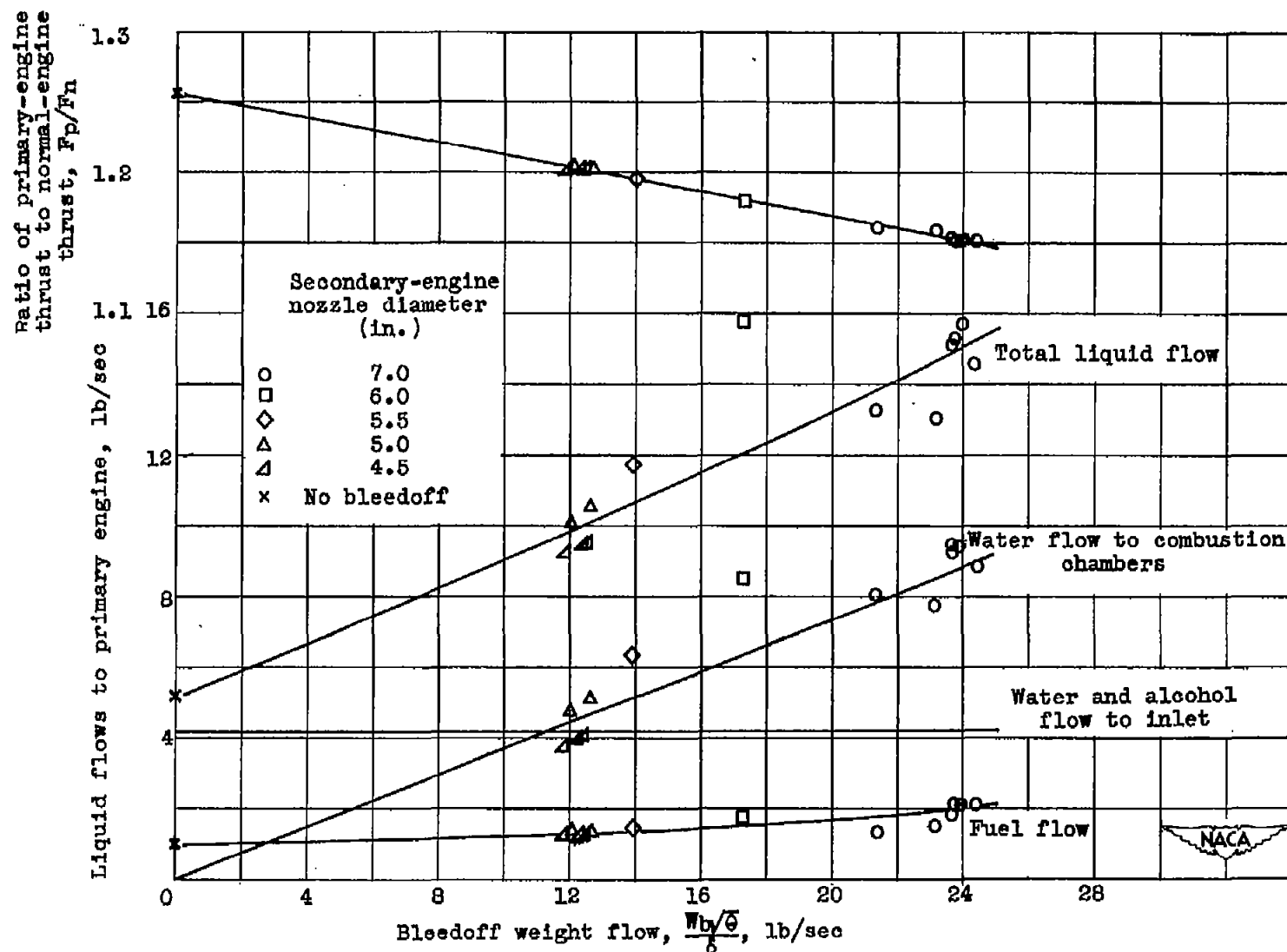
Figure 7. - Variation of individual liquid flows to primary engine and ratio of primary-engine thrust to normal-engine thrust with bleedoff weight flow.
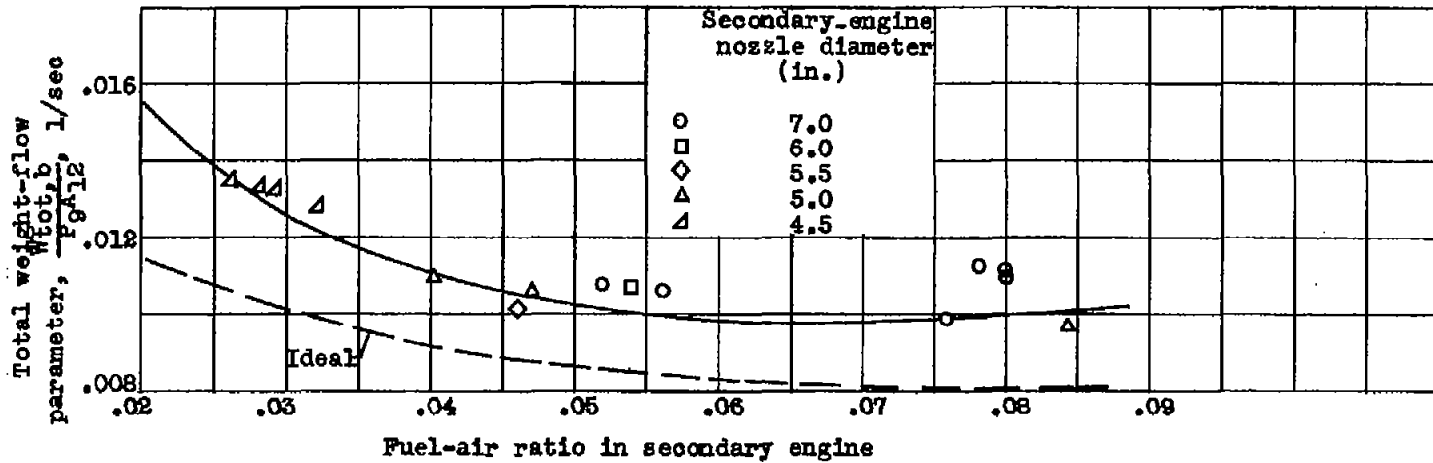
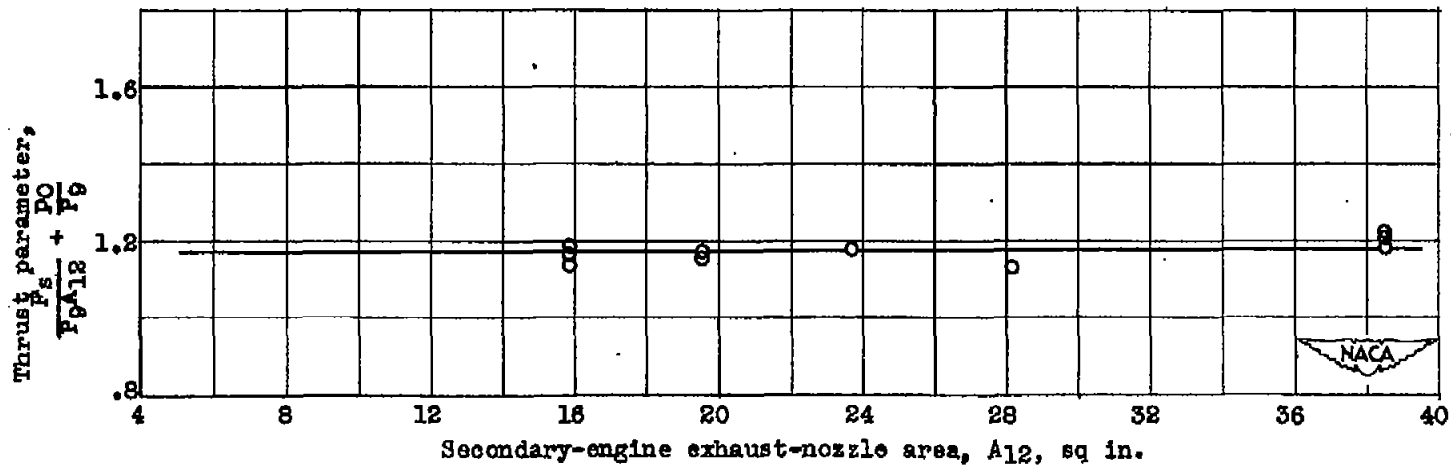Figure 8. - Secondary-engine total-weight-flow parameter as function of secondary-engine fuel-air ratio.

Figure 9. - Variation of secondary-engine thrust parameter with secondary-engine exhaust-nozzle area.
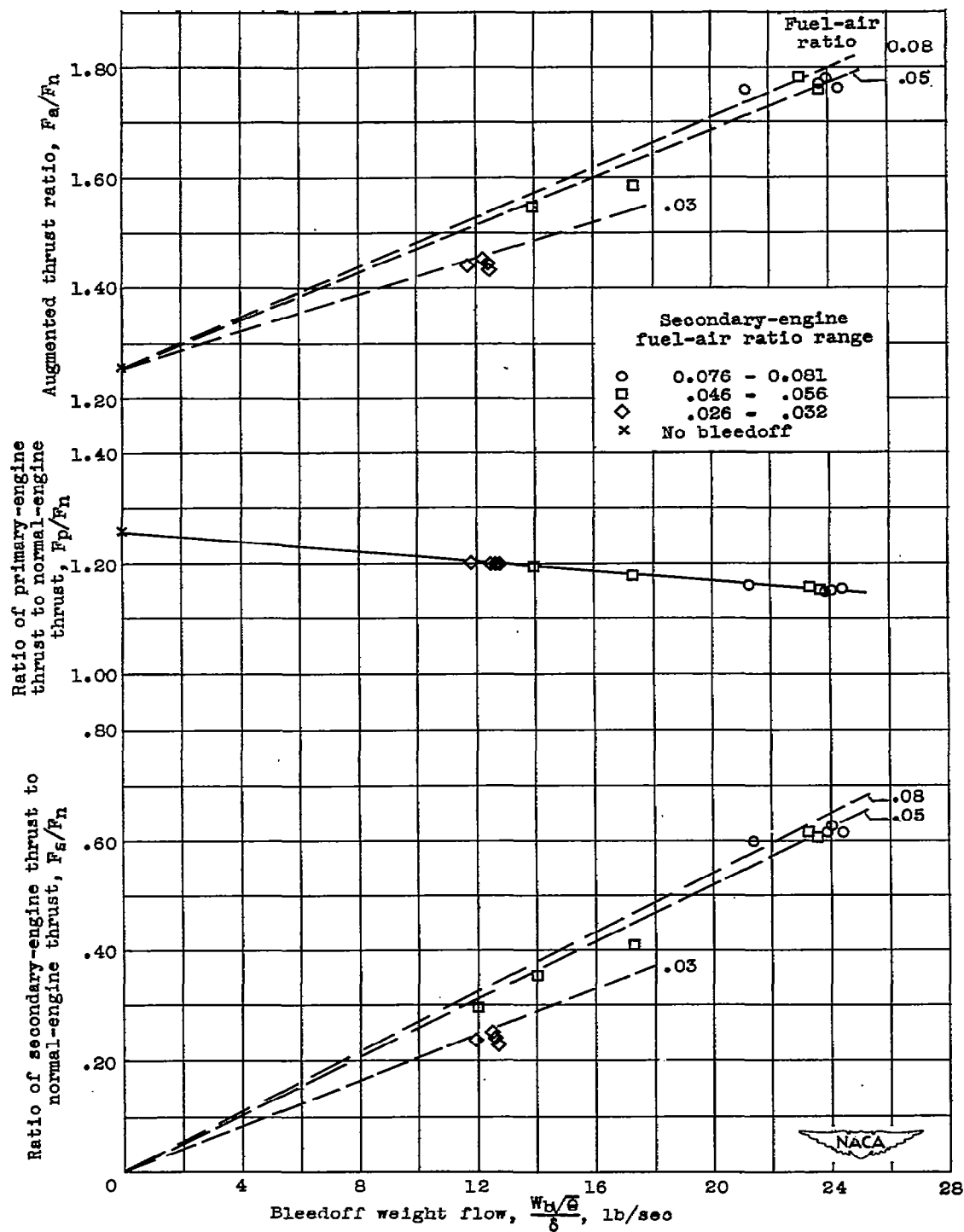
Figure 10. - Variation of primary-engine, secondary-engine and total augmented thrust with bleedoff weight flow for several secondary-engine fuel-air ratio ranges.
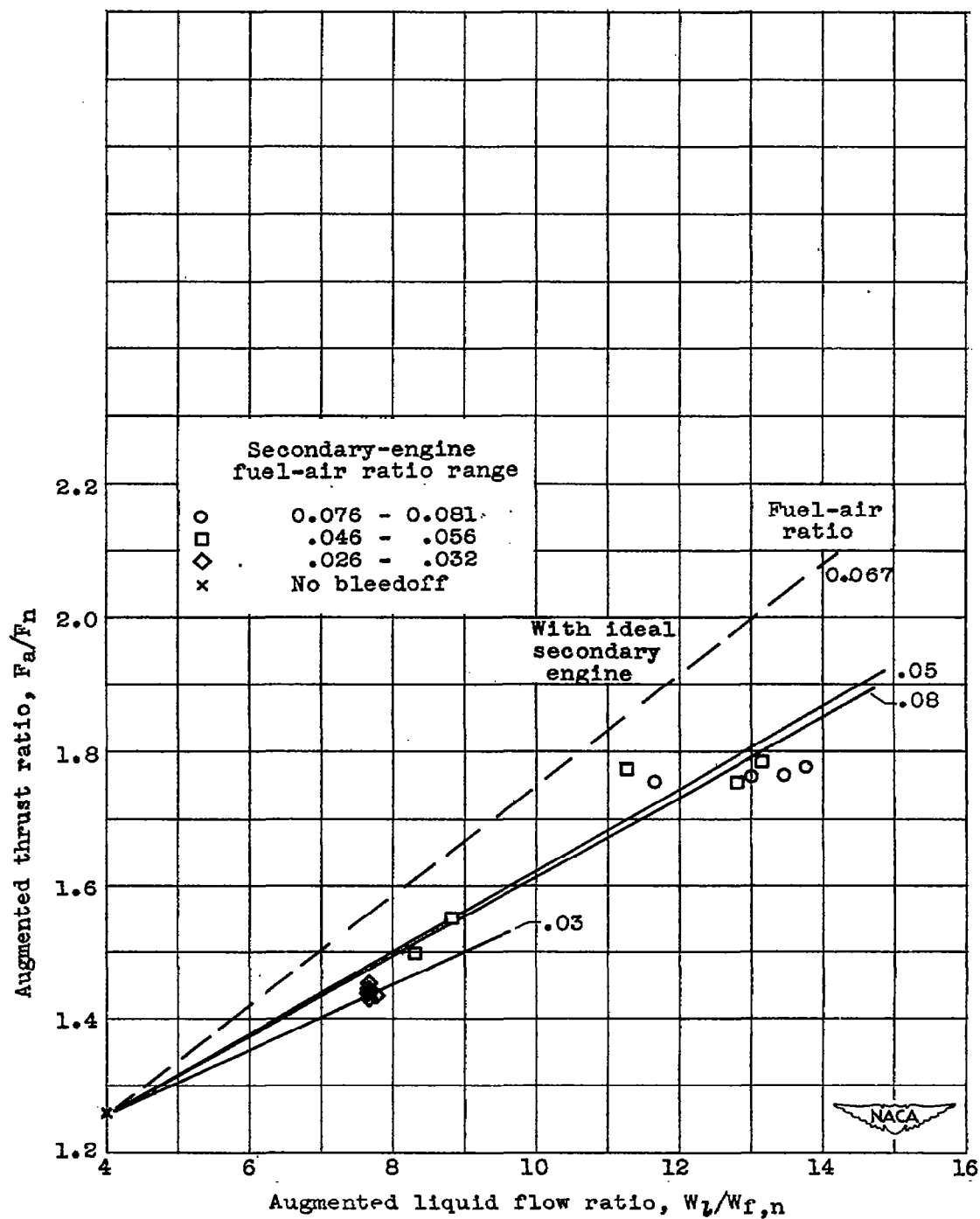
Figure 11. - Variation of augmented thrust ratio with augmented liquid flow ratio.